Egyptian Journal of Chemistry

http://ejchem.journals.ekb.eg/

Shielding Behavior and Structural Role of Bismuth Oxide in Ternary Bismuth Lead Borate Glass

Noha G. Kattaya[a],*, O.M.Hemeda[a], M.S. Meikhail[b], A.M. Abdelghany[c,d] M. M. Ali[a]

[a]*Physics Department, Faculty of Science, Tanta University, Tanta, Egypt*
[c]*Physics Department, Faculty of Science, Mansoura University, 35516, Mansoura, Egypt*
[b]*Spectroscopy Department, Physics Division, National Research Centre, 33 ElBehouth St., Dokki, 12311, Giza, Egypt*
[d]*Basic Science Department, Horus University, International Coastal Road, New Damietta, KafrSaad, Damietta, Egypt*

Abstract

Different concentrations of bismuth oxide (x= 0, 5, 10, 15, 20, 25, 30) are added at the expense of boron oxide in the synthesized glassy matrix containing a fixed concentration of lead oxide. All the prepared samples are characterized using FTIR, UV/Vis. spectroscopic techniques and XRD before and after being exposed to γ-radiation of doses 8 and 12 Mrad. No changes are observed in the wavenumber positions related to the functional groups of the constituents after irradiation. The optical band gap shows a decreasing trend after irradiation that depends on the irradiation dose. The number of coordinate boron reveals a minor variation in their values correlated to the radiation dose. Besides, all glasses show amorphous nature before and after irradiation indicating that samples can be used for radiation shielding.

1. Introduction

B₂O₃ is considered one of the serious former glass and influx materials. It dissolves in high viscosity-rich compositions of B_2O_3 and tends to form glass. The important features of, borates with various compositions are important because of their versatile optical characteristics [1, 2]. Boron oxide can be considered as one of the most prevalent glass-formers which have two different structural units that are arranged or linked with each other to form vitreous structural groups namely [BO₃] triangular units and [BO₄] tetrahedral units depending on the glass composition.

Bismuth oxide is a heavy metal oxide with substantial third-order nonlinear optics susceptibility when used as a conditional glass, forming a higher refractive index combined with higher density within the glassy matrix [3, 4]. Bismuth oxide is also used for the preparation of high-temperature superconducting ceramics having the ability to absorb gamma radiation. The addition of Bi_2O_3 to different glass matrices results in higher corrosion characteristics and low crystallization tendency through crosslinking characteristics resulting from both distorted octahedral [BiO₆] that may act as a network modifier and/or pyramidal [BiO₃] units that act as a glass former within different glass network. The high density and optical transparency of glasses containing heavy metal oxide including bismuth and lead make them ideal for radiation shielding applications besides other optical and optoelectronic applications. Both bismuth and lead ions are used as modifiers in the borate matrix which may result in the lowering of the glass melting temperatures and extension of the glass formation region [5-8].

Gamma rays are considered a part of ionizing radiation that interacts with the material through three different processes. Namely, photoelectric effect, Compton scattering, and pair production depending on the energy of the incident photons. Gamma rays

___

usually produce point defects most of them resulting from the secondary fast electrons while the vacancies in solid materials are mobile and combined with themselves from a complex defect to attain lower energy levels in the forbidden gap [9].

Presented work aims to introduce an optimized glass structure containing different amounts of heavy metal oxide (HMO) that may be used in different radiation applications as a glass shielding or dosimeter. The work extended to study the effect of different additives in the structure and optical characteristics of studied glasses.

2. Experimental Work

Pure chemical materials are used for the glass preparation including Boron oxide (B_2O_3) obtained from Orthoboric acid (H_3BO_3) supplied by El-Nasr chemicals. Lead oxide and bismuth oxide are supplied by Rayasan chemicals and used as received. Melt-quenching method is used for preparation of sample with compositions of $(60-x)B_2O_3$-$40(PbO)$-xBi_2O_3 where ($x = 0.0, 5, 10, 15, 20, 25, 30$). Sample notation and composition are recorded in table (1).

Table (1): Sample notation and composition

Notation	Composition mol%		
	B_2O_3	PbO	Bi_2O_3
PbBBi0	60	40	0.0
PbBBi5	55	40	5
PbBBi10	50	40	10
PbBBi15	45	40	15
PbBBi20	40	40	20
PbBBi25	35	40	25
PbBBi30	30	40	30

For spectroscopic characterization, pulverized glass samples are used for FTIR while polished samples are used for UV/Vis. measurements. All samples are subjected to the same gamma-ray doses (8Mrad and 12Mrad). FTIR spectral data is recorded within full range extended between 4000-400 cm^{-1} using Nicolet i10 ThermoFisher using traditional KBr disc techniques. Minor amounts of pulverized glass sample to KBr (1:100 g) are mixed in an agate mortar and subjected to a pressure of 5 tons/cm^2 until clear homogeneous discs are obtained. FTIR spectral data are recorded immediately after disc preparation to avoid moisture attacks. Polished glass samples with required dimensions are employed to measure the UV/Vis. optical absorption spectra using JASCO V-570 double beam spectrophotometer within the range 200 to 900 nm. All samples are measured before and

after the irradiation process. XRD experimental data is recorded for fine glassy powdered samples via PANalytical X`Pert PRO system adopting copper K_α line in the range 2θ diffraction angle between 4 to 70° to ensure the amorphous nature of the prepared samples and to confirm the absence of any phase separation or tendency for crystallization processes.

3. Results and discussion

3.1. X-ray diffraction

Figures (1-a,b, and c) show the XRD pattern of the studied glasses before and after being irradiated with two different gamma-ray doses namely 8 and 12 Mrad. The lack of a prominent peak establishes the absence of any long-range organization pattern in the crystalline structure [10]. In other words, it proves the glassy attitude of the studied samples before and after irradiation with gamma radiation doses.

3.2. FTIR Spectral Absorption data

Figure (2) shows FTIR spectral absorbance of the prepared glass samples before irradiation. Obtained data shows the general behavior of previously studied lead borate glasses comprising several broad peaks characterizing the presence of both triangular borate units (BO_3) and tetrahedral borate units (BO_4). Introducing heavy metal oxide (Bi_2O_3) may result in some important variations including change in intensity of some peaks and change of wavenumber position of the band originally located at 1320 cm^{-1} is assigned to BO_3 vibration groups. The broad less intense band centered at about 940 cm^{-1} is usually assigned to BO_4 structural unit vibrations [11-13].

The spectra also reveal maintenance of a small peak with a fixed position nearly in all samples located at 695 cm^{-1}. Further addition of HMO results in the generation of a new low-intensity band centered at about 485 cm^{-1} attributed to the presence of Bi_2O_3 oxide with higher contents (15-30 mole%). The same behavior is observed for the samples that irradiated with 8 and 12 Mrad with minor changes. Band assignment and correlation with the experimental data are well estimated and conducted through deconvolution analysis technique (DAT) of the spectral data for smeared and overlapped peaks within the fingerprint region extended from 2000 to 400 cm^{-1} [14].
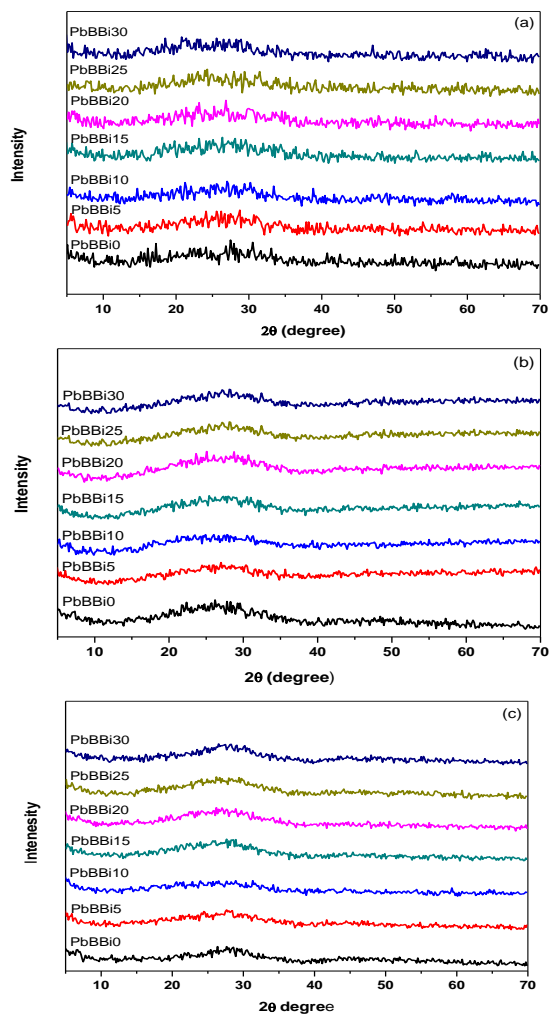
Figure (1): XRD pattern of (a) samples before irradiation (b) samples after 8Mrad gamma irradiation and (c) samples after 12Mrad gamma irradiation
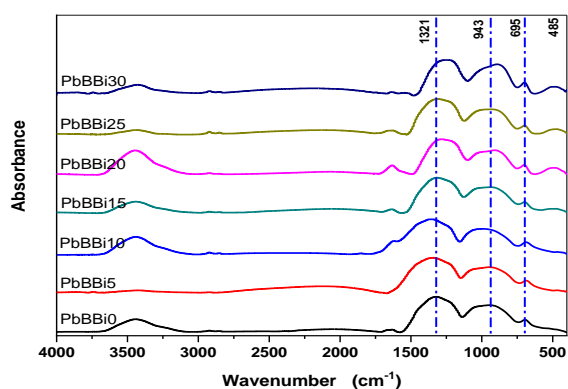

Figure (2): FTIR spectral absorbance of the prepared glass samples before irradiation.

Obtained spectra are corrected for background and dark current noises using the Peak fit 4.12 program while the position of the suggested Gaussian spectral peaks is determined from previous studies of the same base glass in addition to the second derivative of

original spectral data [15, 16]. Obtained data is shown as an example in Figure (3) and employed to calculate the fraction of tetrahedral boron (N4) using the well-known formula:

$$N_4 = \frac{BO_4}{BO_4 + BO_3} \qquad (1)$$

Where BO_3 and BO_4 represent the areas corresponding to both BO_3 and BO_4 structural groups respectively.
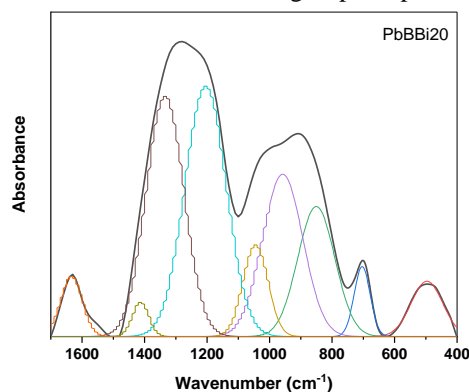

Figure (3): deconvolution analysis for the sample PbBBi20

Table (2) summarizes the analyzed FTIR main spectral bands associated with their assignments.

Additional bands can be observed in lead borate glass resulting from the introduction of lead oxide. Several authors reported that lead can be introduced in the borate matrix as former or modifier oxide based on their content [18]. Therefore, Pb-O-B bending vibrations can be observed in the spectral range 400-650 cm^{-1}. In addition, it is noticed that different irradiation doses generate minor variations in the intensities of the characteristic peaks without any change in their position indicating that gamma irradiation does is not effective on the structural building units and the changes in FTIR bands may result from the rearrangement of the building units. Figures (4-a,b) show an example of FTIR for parent glass sample and samples that contain 25 mol% Bismuth oxide before and after being irradiated with two different doses (8 and 12 Mrad)

The deconvolution analysis technique (DAT) is used again to calculate the fraction of four coordinated boron and to retrace the structural changes associated with the irradiation processes. Calculated data are listed in the table (3) and shown in Figure (5).

Noha G. Kataya et.al.

_____

Table (2): FTIR spectral bands of studied borate units associated with their assignments

Wavenumber (cm⁻¹)	Assignment	Ref.
600-800	BO_3 bending stretching of trigonal BO_3 groups	**11-14**
800-1200	B–O–B (and Pb–O–B) bending and borate ring deformation of BO_4 units	**13, 15**
1200-1600	BO_3 stretching vibrations of trigonal BO_3 units	**13, 15, 18**
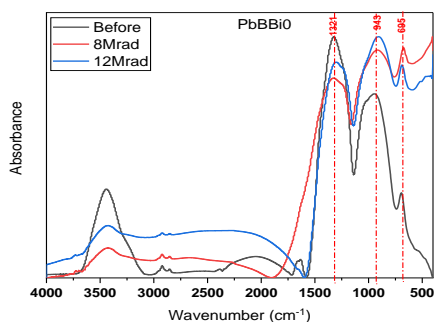
(a)
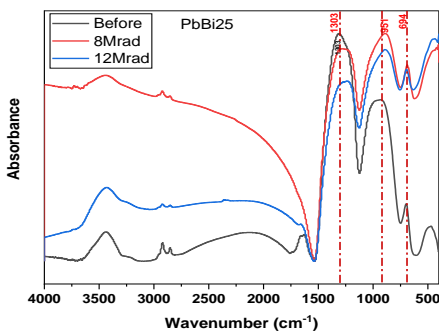
(b)

Figures (4-a,b): FTIR spectra of parent glass and samples that contain 25 mol% Bismuth oxide before and after gamma irradiation

Table (3): fraction of the four coordinated boron before and after irradiation

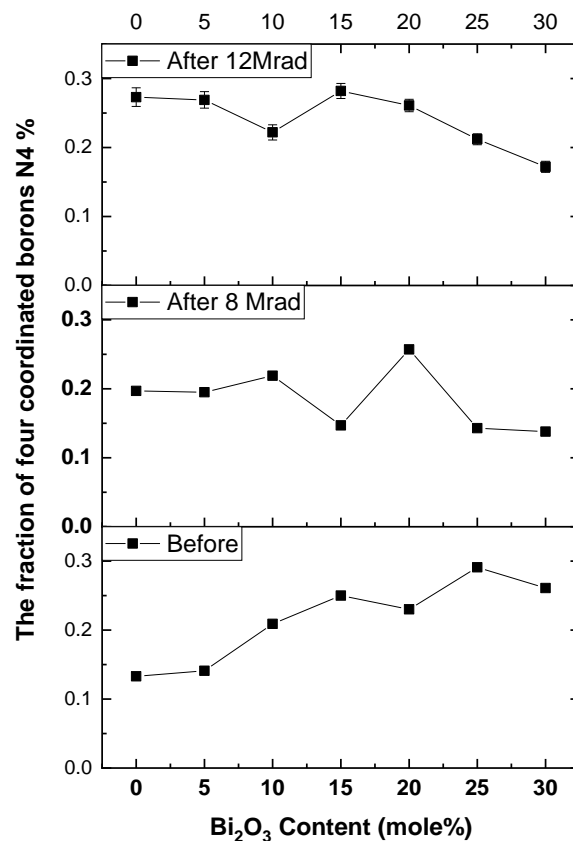| Sample	Bi₂O₃ Content	N4		
		Before	**After 8Mrad**	**After 12 Mrad**
PbBBi0	٠	٠,١٣٣	٠,١٩٧	٠,٢٧٣
PbBBi5	٥	٠,١٤١	٠,١٩٥	٠,٢٦٩
PbBBi10	١٠	٠,٢٠٩	٠,٢١٩	٠,٢٢٢
PbBBi15	١٥	٠,٢٥	٠,١٤٧	٠,٢٨٢
PbBBi20	٢٠	٠,٢٣	٠,٢٥٧	٠,٢٦١
PbBBi25	٢٥	٠,٢٩١	٠,١٤٣	٠,٢١٢
PbBBi30	٣٠	٠,٢٦١	٠,١٣٨	٠,١٧٢

Figure (5): fraction of the four coordinated boron before and after irradiation.

Distortion for both kinds of unit's borate is between 600 and 800 cm⁻¹. Bands with the range 200-400 cm⁻¹ explained the last region and these bands are specified to cations metal vibrations at their sites. The existence of dense structural units made up of interconnected BO_4 and BO_3 groups, as well as heavy Bi^3 cations such as BiO_3 and/or BiO_6 units, display shielding properties against successive gamma irradiation. The presence of Bi_2O_3 and B_2O_3 together reveals the appearance of BO_4 vibrational bands at about 950 and 1100 cm⁻¹ due to the sharing of oxygen from Bi_2O_3 to form tetrahedral BO_4 groups. The absorption band at 695 cm⁻¹ indicates the presence of BO_3. The absorption band at 943 cm⁻¹ coincides with the BO_4 vibration groups that from Bi–O vibrations which lie in the same position [18].

3.3 UV/Visible Spectral Absorption data

Figure (6) shows UV/Vis. spectral absorption data of the prepared glassy samples before irradiation
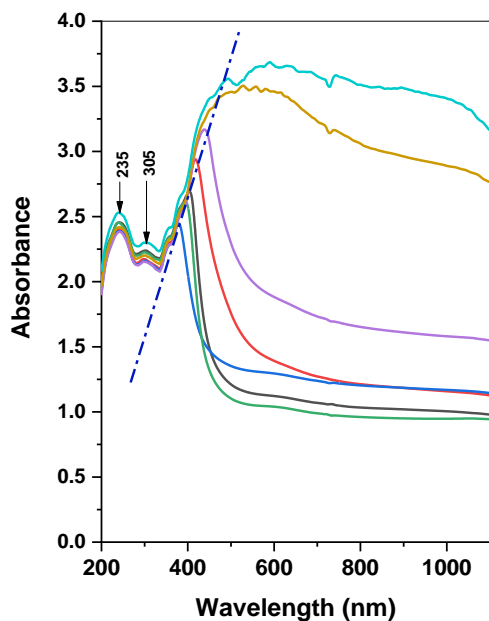
_____

Figure (6) UV/Vis. spectral absorption data of the studied glasses

The spectral data shows the presence of a prominent peak located at 235 nm in all samples originally attributed for the presence of unavoidable trace impurity of iron from the chemicals used in the preparation of refractory when melted. Such band is followed by another weak band at 305 nm and combined with a more intense band with a shoulder whose peak shifts from 380 to 485 nm due to the increasing of bismuth content pointing to the expected changes in the values of the optical energy gap. The UV-near visible absorption bands in the range 275–440 nm are observed in high bismuth borate or high-bismuth silicate glasses and correlated to Bi^{+3} ions [19].

Abdelghany et al. [20, 21] and Ehrt et al [22, 23] confirmed this postulation that characterizes the absorption of charge transfer in un-doped alkali phosphate glass. Some metal ions (such as Pb^{2+} and Bi^{3+}) are thought to absorb radiation during electronic transitions involving the metal ions orbitals, and such spectra have been given the term "Rydberg." Duffy [24] investigated the absorbed ultraviolet in lead glasses and proposed that lead ions (Pb^{2+}) play a role in UV absorption generation in such glasses. Therefore, the optical energy gap is calculated for both direct allowed and indirect allowed transition using Davis and Mott's equation describing the absorption coefficient α as a function of frequency ν [25]:

$$\alpha(\nu)h\nu = B(h\nu - E_{gap})^m \qquad (2)$$

Where B, $h\nu$ and E_{gap}, are a constant, the photon energy and the energy gap respectively while the

power m is a constant characterize the type of transition concerning the momentum space. The values of the optical energy gap are estimated by plotting the photon energy versus $(\alpha h\nu)^2$ for the indirect allowed transitions as shown in the spectrum of base glass and glass containing 25 mol% bismuth oxide as exemplified in Figures (7. a, b).
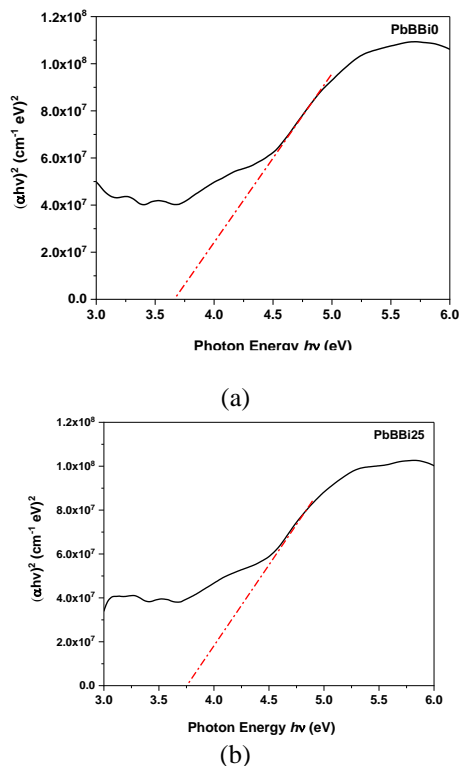

(a)

(b)

Figure (7) photon energy versus $(\alpha h\nu)^2$ for the indirect allowed transitions

The same calculations are made after the samples are irradiated with two different doses of gamma rays, namely 8 and 12 Mrad as shown in figure (8), while the obtained data is tabulated in table 4.

From the previous data, it is clear that both density and optical energy gap can be considered as a function of bismuth concentration, and increasing bismuth content results in an increase in both density and optical energy gap resulting from the fact that bismuth replaces boron. In addition, it is observed that the optical energy gap is sensitive to gamma-ray radiation doses and the optical energy gap is reduced with increasing radiation doses as a result of the rearrangement of structural units as previously discussed by different authors [26, 27].
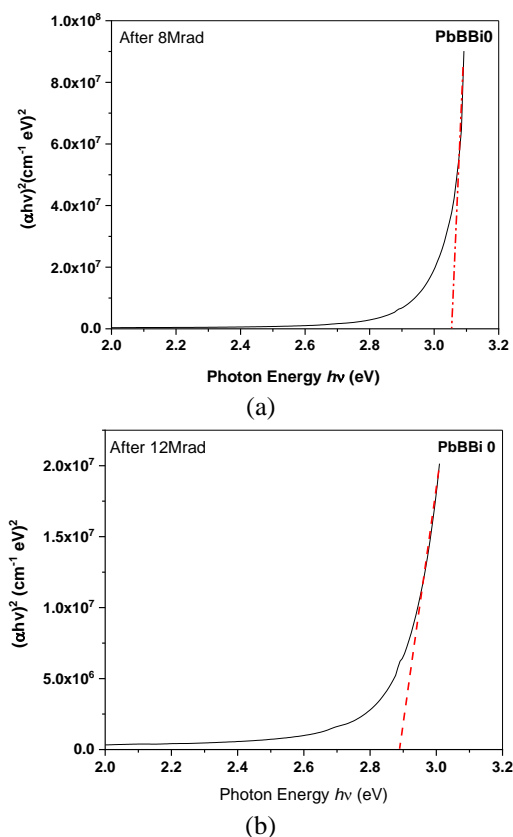
(a)

(b)

Figure (8): photon energy versus $(\alpha h\nu)^2$ for gamma-irradiated samples

Table (4): density and Optical energy gap before and after radiation.

Sample	Density (g/cm³)	Optical energy gap (eV)		
		Before	After 8Mrad	After 12 Mrad
PbBBi0	5.66	3.38	3.22	2.89
PbBBi5	5.64	3.43	3.27	2.97
PbBBi10	5.92	3.49	3.35	3.02
PbBBi15	6.36	3.57	3.42	3.15
PbBBi20	6.11	3.63	3.50	3.21
PbBBi25	6.24	3.75	3.58	3.28
PbBBi30	6.11	3.84	3.66	3.31

It is already known that the exposition of glasses to high-energy radiation (X-ray, γ-rays, ultraviolet light) gives various features such as chemical, optical, electrical, magnetic, and mechanical properties [28]. Gamma rays may result in a change in the UV/Vis. electronic transitions resulting from centers that generated due to capturing liberated pairs of electrons and positive holes through a radiation process pointing to the shielding attitude of the studied samples [29].

4. Conclusion

Sample of the ternary glass system composed of lead-bismuth borate including bismuth at expense of boron atoms is successfully synthesized using the traditional melt quenching route. Prepared samples are studied using spectroscopic techniques before and after irradiation with two different gamma-ray doses to retrace the effect of both irradiation doses and bismuth content. FTIR Spectral data shows the maintenance of the absorption bands related to both trigonal BO_3 and tetrahedral BO_4 units. Calculations of the four coordinated boron N4 before and after gamma irradiation reveal that the number of four coordinated boron increases with increasing both bismuth content and irradiation doses. Bismuth addition is noticed to introduce limited variations due to the formation of extra structural causing some polymerization.

5. References

1. Madshal, M. A., El-Damrawi, G., Abdelghany, A. M., & Abdelghany, M. I. (2021). Structural studies and physical properties of Gd 2 O 3-doped borate glass. *Journal of Materials Science: Materials in Electronics*, 1-12. https://doi.org/10.1007/s10854-021-06022-1

2. Kamitsos, E. I., Patsis, A. P., Karakassides, M. A., & Chryssikos, G. D. (1990). Infrared reflectance spectra of lithium borate glasses. *Journal of Non-Crystalline Solids*, *126*(1-2), 52-67. https://doi.org/10.1016/0022-3093(90)91023-K

3. Chen, Q. (2020). Optical linear & nonlinearity and Faraday rotation study on V_2O_5 nanorod doped glass and glass-ceramic: impact of optical basicity. *Journal of Alloys and Compounds*, *836*, 155490. https://doi.org/10.1016/j.jallcom.2020.155490

4. Rammah, Y. S., Ali, A. A., El-Mallawany, R., & Abdelghany, A. M. (2019). Optical properties of bismuth borotellurite glasses doped with NdCl3. *Journal of Molecular Structure*, *1175*, 504-511. https://doi.org/10.1016/j.molstruc.2018.07.071

5. Hammad, A. H., Abdelghany, A. M., & ElBatal, H. A. (2017). Thermal, structural, and morphological investigations of modified bismuth silicate glass-ceramics. *Silicon*, *9*(2), 239-248. https://doi.org/10.1007/s12633-016-9433-9

6. Singh, N., Singh, K. J., Singh, K., & Singh, H. (2004). Comparative study of lead borate and bismuth lead borate glass systems as gamma-radiation shielding materials. *Nuclear Instruments and Methods in Physics Research Section B: Beam Interactions with Materials and Atoms*, *225*(3), 305-309. https://doi.org/10.1016/j.nimb.2004.05.016

7. Lakshminarayana, G., Kumar, A., Tekin, H. O., Issa, S. A., Al-Buriahi, M. S., Dong, M. G., ... & Park, T. (2021). In-depth survey of nuclear radiation attenuation efficacies for high density bismuth lead borate glass system. *Results in Physics*, *23*, 104030. https://doi.org/10.1016/j.rinp.2021.104030

8. Sangeeta, B. K., & Ayachit, N. H. (2021, March). Density, Molar Volume and IR Studies of Lithium Doped Bismuth Lead Borate Glasses. In *IOP Conference Series: Materials Science and Engineering* (Vol. 1126, No. 1, p. 012065). IOP Publishing. https://doi.org/10.1088/1757-899X/1126/1/012065

9. Diab, H. M., Abdelghany, A. M., & Hafez, H. S. (2020). Dosimetric behavior of modified borate bioglass containing copper for low photon dose measurements using luminescence characteristics. *Journal of Materials Science: Materials in Electronics*, *31*(22), 20452-20459. https://doi.org/10.1007/s10854-020-04564-4

10. Abou Hussein, E. M., Maksoud, M. A., Fahim, R. A., & Awed, A. S. (2021). Unveiling the gamma irradiation effects on linear and nonlinear optical properties of CeO_2–Na_2O–SrO–B_2O_3 glass. *Optical Materials*, *114*, 111007. https://doi.org/10.1016/j.optmat.2021.111007

11. Ali, A. A., Rammah, Y. S., El-Mallawany, R., & Souri, D. (2017). FTIR and UV spectra of pentaternary borate glasses. *Measurement*, *105*, 72-77. https://doi.org/10.1016/j.measurement.2017.04.010

12. Kashif, I., & Ratep, A. (2021). ICMMS-2: Influences the Addition of Neodymium Oxide on Structural and Optical Properties of Oxyfluoride Lead Borate Glass. *Egyptian Journal of Chemistry*, *64*(3), 1141-1147. https://doi.org/ 10.21608/ejchem.2021.55860.3183

13. Nagaraju, R., Devaiah, B., Haritha, L., Sekhar, K. C., Shareefuddin, M., Sayed, M. A., ... & Kumar, K. V. (2021). Influence of CaF_2 on spectroscopic studies of lead fluoro bismuth borate glasses doped with Cr^{3+} ions. *Journal of Non-Crystalline Solids*, *560*, 120705. https://doi.org/10.1016/j.jnoncrysol.2021.120705

14. Abdelghany, A. M. (2010). The elusory role of low level doping transition metals in lead silicate glasses. *Silicon*, *2*(3), 179-184. https://doi.org/10.1007/s12633-010-9053-8

15. Gaafar, M. S., Marzouk, S. Y., Mahmoud, I. S., Henda, M. B., Afifi, M., Abd El-Aziz, A. M., & Alhabradi, M. (2020). Role of Neodymium on Some Acoustic and Physical Properties of Bi_2O_3-B_2O_3-SrO Glasses. *Journal of Materials Research and Technology*, *9*(4), 7252-7261. https://doi.org/10.1016/j.jmrt.2020.04.086

16. Abdelghany, A. M., & Rammah, Y. S. (2021). Transparent alumino lithium borate glass-ceramics: synthesis, structure and gamma-ray shielding attitude. *Journal of Inorganic and Organometallic Polymers and Materials*, *31*(6), 2560-2568. https://doi.org/10.1007/s10904-020-01862-6

17. Varsamis, C. P. E., Makris, N., Valvi, C., & Kamitsos, E. I. (2021). Short-range structure, the role of bismuth and property–structure correlations in bismuth borate glasses. Physical Chemistry Chemical Physics, 23(16), 10006-10020. https://doi.org/10.1039/D1CP00301A

18. Griebenow, K., Muñoz, F., Tagiara, N. S., Klement, R., Prnová, A., Wolfrum, B., ... & Galusek, D. (2021). Structure and fluorescence properties of Dy-doped alkaline-earth borophosphate glasses. International Journal of Applied Glass Science. https://doi.org/10.1111/ijag.16105

19. Doweidar, H., & Saddeek, Y. B. (2009). FTIR and ultrasonic investigations on modified bismuth borate glasses. *Journal of Non-Crystalline Solids*, *355*(6), 348-354. https://doi.org/10.1016/j.jnoncrysol.2008.12.008

20. Abdelghany, A. M., & Margha, F. H. (2016). New Transparent Nano-Glass-Ceramics of SiO_2 and CaF_2 doped SrO-B_2O_3 Glass. *Silicon*, *8*(4), 563-571. https://doi.org/10.1007/s12633-014-9277-0

21. ElBatal, F. H., Marzouk, M. A., & Abdelghany, A. M. (2011). UV–visible and infrared absorption spectra of gamma irradiated V_2O_5-doped in sodium phosphate, lead phosphate, zinc phosphate glasses: a comparative study. *Journal of non-crystalline solids*, *357*(3), 1027-1036. https://doi.org/10.1016/j.physb.2011.06.074

22. Ehrt, D., Ebeling, P., & Natura, U. (2000). UV Transmission and radiation-induced defects in phosphate and fluoride–phosphate glasses. *Journal of Non-Crystalline Solids*, *263*, 240-250. https://doi.org/10.1016/S0022-3093(99)00681-X

23. Möncke, D., & Ehrt, D. (2004). Irradiation induced defects in glasses resulting in the photoionization of polyvalent dopants. *Optical Materials*, *25*(4), 425-437. https://doi.org/10.1016/j.optmat.2003.11.001

24. Calas, G., Galoisy, L., & Cormier, L. (2021). The Color of Glass. Encyclopedia of Glass Science, Technology, History, and Culture, 1, 677-691. https://doi.org/10.1002/9781118801017.ch6.2

25. Davis, E. A., & Mott, N. (1970). Conduction in non-crystalline systems V. Conductivity, optical absorption and photoconductivity in amorphous semiconductors. *Philosophical magazine*, *22*(179), 0903-0922. https://doi.org/10.1080/14786437008221061

26. Chopra, N., Singh, N. P., Baccaro, S., & Sharma, G. (2012). UV–vis spectroscopic Investigation on γ-irradiated alkali aluminoborate glasses. *Physica B: Condensed Matter*, *407*(8), 1209-1213. https://doi.org/10.1016/j.physb.2012.01.096

27. Ibrahim, M., ElBatal, H. A., Abdelghany, A. M., Fanny, M., & Hassaan, M. Y. (2021). ICMMS-2: Gamma-rays interactions on the spectral properties of CuO-doped lithium host barium borate glasses. *Egyptian Journal of Chemistry*, *64*(3), 7-8. https://doi.org/10.21608/ejchem.2021.55869.3186

28. Wantana, N., Kaewnuam, E., Kim, H. J., Kang, S. C., Ruangtaweep, Y., Kothan, S., & Kaewkhao, J. (2020). X-ray/proton and photoluminescence behaviors of Sm3+ doped high-density tungsten gadolinium borate scintillating glass. *Journal of Alloys and Compounds*, *849*, 156574. https://doi.org/10.1016/j.jallcom.2020.156574

29. Wang, T. T., Zhang, X. Y., Sun, M. L., Du, X., Guan, M., Peng, H. B., & Wang, T. S. (2020). γ-Irradiation effects in borosilicate glass studied by EPR and UV–Vis spectroscopies. *Nuclear Instruments and Methods in Physics Research Section B: Beam Interactions with Materials and Atoms*, *464*, 106-110. https://doi.org/10.1016/j.nimb.2019.12.007